ACS APPLIED MATERIALS & INTERFACES

Research Article

www.acsami.org

Potential-Modulated Electrochemiluminescence of Carbon Nitride Nanosheets for Dual-Signal Sensing of Metal Ions

Qiuwei Shang,[†,§] Zhixin Zhou,[†,§] Yanfei Shen,[‡] Yuye Zhang,[†] Ying Li,[†] Songqin Liu,[†] and Yuanjian Zhang*[,†]

[†]Jiangsu Province Hi-Tech Key Laboratory for Bio-Medical Research, Jiangsu Optoelectronic Functional Materials and Engineering Laboratory, School of Chemistry and Chemical Engineering, Southeast University, Nanjing 211189, China

[‡]Medical School, Southeast University, Nanjing 210009, China

Supporting Information

ABSTRACT: As an emerging semiconductor, graphite-phase polymeric carbon nitride (GPPCN) has drawn much attention not only in photocatalysis but also in optical sensors such as electrochemiluminescence (ECL) sensing of metal ions. However, when the concentrations of interfering metal ions are several times higher than that of the target metal ion, it is almost impossible to distinguish which metal ion changes the ECL signals in real sample detection. Herein, we report that the dual-ECL signals could be actuated by different ECL reactions merely from GPPCN nanosheets at anodic and cathodic potentials, respectively. Interestingly, the different metal ions exhibited distinct quenching/enhancement of the ECL signal at different driven potentials, presumably ascribed to the diversity of energy-level matches between the metal ions and GPPCN nanosheets and catalytic interactions of the intermediate species in ECL reactions. On this basis, without any labeling and masking reagents, the accuracy and reliability of sensors based on the ECL of GPPCN nanosheets toward metal ions were largely improved; thus, the false-positive result caused by interferential metal ions could be effectively avoided. As an example, the proposed GPPCN ECL sensor with a detection limit of 1.13 nM was successfully applied for the detection of trace Ni^{2+} ion in tap and lake water.

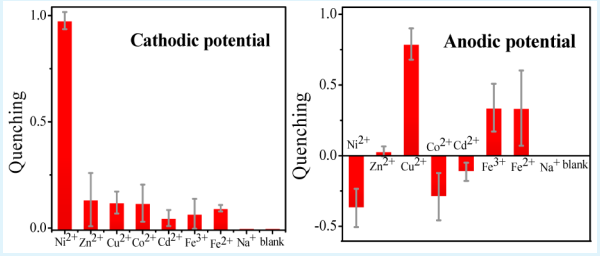

KEYWORDS: *carbon nitride nanosheets, electrochemiluminescence, single luminophor, dual-signal sensing, potential resolved*

INTRODUCTION

Accurate and reliable detection of metal ions is thoroughly significant given the essential relationship with human health and ecosystems.[1] For instance, an insufficient or excess amount of Ni^{2+} ion in the human body may lead to body dysfunctions or DNA damage and lung cancer.[2,3] Among various techniques, electrochemiluminescence (ECL) sensing that largely relies on the property of luminophors provides merits of high sensitivity, high range response, low background noise, and instrument simplicity.[4−8] As an emerging polymeric semiconductor, graphite-phase polymeric carbon nitride (GPPCN) with a layered two-dimensional (2D) structure has attracted wide attenion not only in (photo)catalysis[9−12] and photovoltaic conversion[13] but also as a luminophor for optical sensors,[14−27] owing to its unique properties.[28] For instance, both cathodic and anodic ECL sensors of GPPCN have been reported individually very recently,[17,18] overcoming several drawbacks of traditional ECL luminophors, such as difficult labeling for ruthenium complexes[29−31] and luminol,[32,33] environmental toxicity or low biocompatibility for metal-containing quantum dots,[29,34] and uncertainty of the luminescent mechanism for carbon dots.[35−37] In contrast, GPPCN is inexpensive compared with the above-depicted,[13,28] fairly biocompatible,[38] and stable-band-gap luminescent emission.[39] In this regard, it is very promising to develop GPPCN as a new candidate to complement traditional ECL luminophors in the analysis field.

GPPCN-based ECL sensors exhibit an interesting selectivity to specific metal ions.[17] However, for practical applications, some factors of the environment such as other metal ions will significantly interfere with the detection result to the target ion, and the false-positive or -negative result may occur merely on a single signal. In general, developing multiple-ECL-signal detection would be a feasible way to effectively restrain the signal interference and improve the accuracy. Although dual-ECL-signal sensors have been proposed, most of them were based on two luminophors or label techniques.[40] Herein, we report that dual-ECL signals based on a single GPPCN luminophor could be actuated by two different ECL reactions of GPPCN nanosheets, at merely anodic or cathodic potentials, respectively. Strikingly, the metal ions exhibited distinct quenching/enhancement of the ECL signal at different driven potentials. On the basis of the preliminary "fingerprint" (ECL quenching or enhancement at cathodic and anodic potentials, respectively) and the linear relationship between the ECL

Received: August 12, 2015
Accepted: October 5, 2015
Published: October 5, 2015

DOI: 10.1021/acsami.5b07405
ACS Appl. Mater. Interfaces 2015, 7, 23672−23678

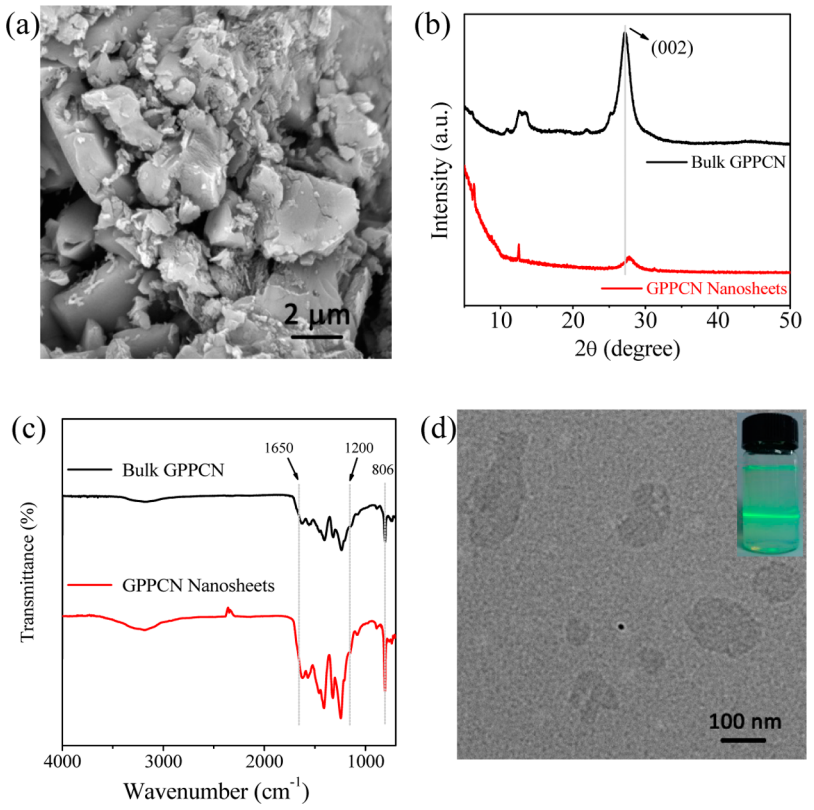

Figure 1. SEM image of bulk GPPCN (a), XRD patterns (b), and FTIR spectra (c) of bulk GPPCN and GPPCN nanosheets and TEM image of GPPCN nanosheets (d). Inset: Tyndall effect of the nanosheets.

intensity and different concentrations of the metal ions, the accuracy and reliability of GPPCN-based ECL sensors were largely improved without labeling and masking reagents. It should be noted that, although in pioneering work it was demonstrated that the applied potential can be exploited to selectively elicit ECL (also called potential resolved ECL) within a single luminophor,[41,42] few ECL sensors, especially those based on GPPCN, have been successfully developed based on this principle so far.[8] The proposed strategy of modulating multiple-ECL signals of GPPCN would pave more reliable and promising applications of carbon-rich materials in sensing and other essential state-dependent responses.

EXPERIMENTAL SECTION

Materials and Reagents. KCl, tris(hydroxymethyl)aminomethane, HCl (37%), and $K_2S_2O_8$ were purchased from Sinopharm Chemical Reagent Co. Ltd. (Shanghai, China). Dicyandiamide and Nafion (10 wt % in water) were purchased from Sigma-Aldrich Co. Ltd. (USA). Triethanolamine (TEA; 98%) was obtained from Aladdin Co. Ltd. (Shanghai, China). Ultrapure water (18.2 MΩ cm) was obtained from a Thermal water purification system. Unless otherwise specified, other chemicals were of analytical grade and were used without further purification.

Characterization. Scanning electron microscopy (SEM) images were carried out on a Phenom ProX scanning electron microscope (The Netherlands). Transmission electron microscopy (TEM) images were measured on a JEM-2100 field-emission electron microscope (Japan) at an acceleration voltage of 200 kV. UV−vis absorption spectroscopy was taken on a Cary series 100 UV−vis spectrophotometer (Agilent, Singapore) with a diffuse-reflectance accessory, and $BaSO_4$ was used as the reference sample (100% reflectance). Powder X-ray diffraction (XRD) was characterized with a Bruker D8 Advance diffractometer (Germany) equipped with high-intensity Cu Kα radiation (λ = 1.54178 Å). Photoluminescence was performed with a fluorescence spectrometer (Fluoromax-4, Horiba Jobin Yvon, Japan). Fourier transform infrared (FTIR) spectroscopy was carried out on a Nicolet 4700 FTIR spectrometer (Thermo, USA), equipped with attenuated total reflectance detector. Electrochemiluminescence (ECL) was performed on a conventional three-electrode quartz cell with a platinum wire as the auxiliary electrode and a calomel electrode (saturated KCl) as the reference electrode with an ECL analyzer system (MPI-E, Xi'anruimai Analytical Instruments Co. Ltd., China). The working electrode was a bare or modified glassy carbon electrode (GCE; d = 3 mm). The ECL intensity in a blank solution was defined as I_0, and the ECL intensity after the addition of a certain concentration of metal ions into the blank solution was defined as I_1. Then, the changes of ECL were calculated by $(I_0 - I_1)/I_0$ to eliminate the interference from trace metal ions in the ultrapure water (18.2 MΩ cm).[14,15,17] Moreover, the definition of ECL changes of $(I_0 - I_1)/I_0$ at a modified electrode made the influence of variances of the absolute ECL intensity at different modified electrodes negligible on the sensing reproducibility. Besides, each measurement after the addition of metal ions was performed independently three times, and the error bars are given.

Synthesis of Bulk GPPCN and GPPCN Nanosheets. Briefly, bulk GPPCN was prepared by placing dicyandiamide in an alumina crucible with a cover, heating for 4 h to 500 °C, and then maintaining this temperature for another 4 h. After that, the obtained yellow agglomerates were ground into fine powders. For the preparation of GPPCN nanosheets, 100 mg of the obtained bulk GPPCN powder was exfoliated in 100 mL of water in a ultrasonic cleaner (300 W) for approximately 16 h and centrifuged at 5000 rpm to remove unexfoliated large GPPCN particles.[38]

Preparation of the GPPCN-Nanosheet-Modified GCE. The GCE was polished to a mirror finish with a 0.03 μm alumina slurry followed by ultrasonication in water. Then the GCE was dried in a N_2 atmosphere, followed by the dropping of 20 μL of GPPCN nanosheets (ca. 0.15 mg/mL) onto its surface and drying in air at room temperature. To stabilize GPPCN nanosheets on the GCE surface and

DOI: 10.1021/acsami.5b07405
ACS Appl. Mater. Interfaces 2015, 7, 23672−23678

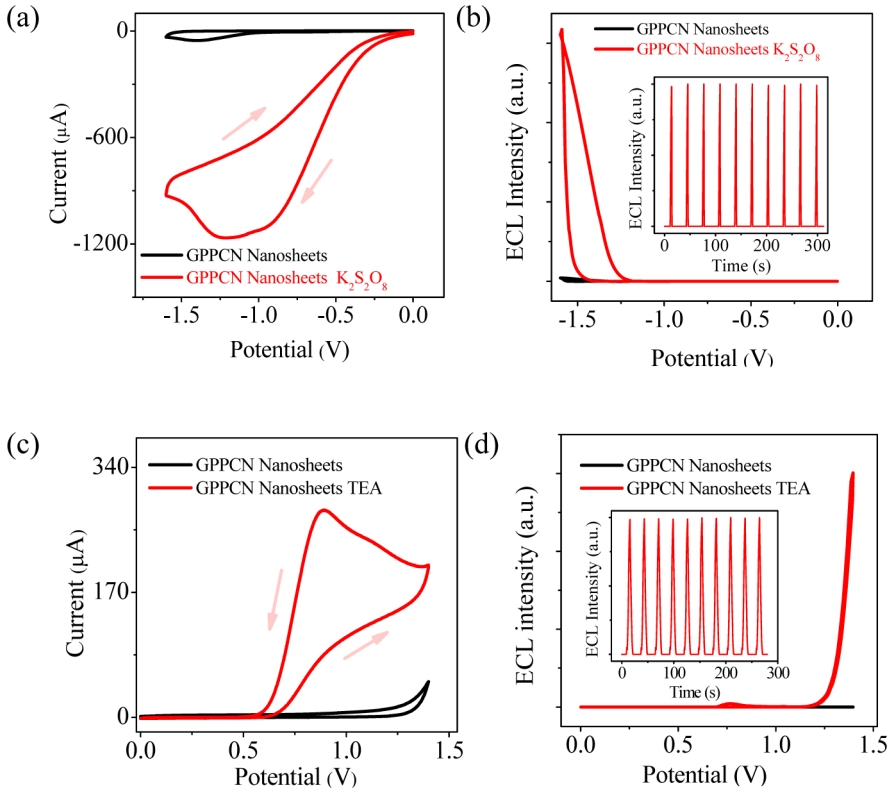

Figure 2. Cyclic voltammetric (a and c) and ECL intensity potential (b and d) curves of the GPPCN-nanosheet-modified GCE of sequential voltage scans between 0 and −1.6 V (a and b) with/without 150 mM $K_2S_2O_8$ and between 0 and 1.4 V (c and d) with/without 60 mM TEA. The electrolyte was 0.01 M Tris-HCl (pH 7.4) containing 0.1 M KCl, and the scanning rate was 100 mV/s. Insets: ECL stability of the as-prepared GPPCN-nanosheet-modified GCE by 10 cycles of sequential voltage scans.

ECL signals as well, 15 μL of Nafion (0.05 wt %) was further dropped onto the surface of GPPCN nanosheets at the GCE and dried in air at room temperature.

RESULTS AND DISCUSSION

Bulk GPPCN was a powder with an average size of around several microns (Figure 1a), and such a powder did not favor the formation of stable films on the GCE and effective charge transfer[43] for ECL studies in aqueous electrolytes because of the apparent grain boundary effects. In general, reducing the particle size is a feasible way to solve this problem. For this, GPPCN nanosheets were successfully prepared by exfoliation of bulk GPPCN in water (see details in the Experimental Section and UV−vis absorption and photoluminescent emission spectra in Figure S1a,b). The texture of the as-prepared GPPCN nanosheets was first assessed by XRD and FTIR spectroscopy. The most typical (002) diffraction peaks at a 2θ of 27° corresponding to the layered stacking 2D structure[44−46] (Figure 1b) and the vibrations at 806 and 1200−1650 cm^{-1} (Figure 1c) corresponding to the primary tri-*s*-triazine units[45] of GPPCN nanosheets were generally retained in comparison with pristine bulk GPPCN. However, the (002) diffraction peak of GPPCN nanosheets was remarkably weaker and slightly shifted to a higher degree in comparison with pristine GPPCN, implying that GPPCN was exfoliated. This was further supported by the observation of ultrathin nanosheets in the TEM image (Figure 1d). The equivalent diameter of the nanosheets (~70−200 nm) was much smaller than that of bulk GPPCN. Moreover, an obvious Tyndall effect of the as-prepared nanosheets (the inset of Figure 1d) was observed, indicating that GPPCN nanosheets could be well-dispersed as colloids in aqueous solution, which was preferred for a uniform and robust film on GCE in practical applications.

Although both bulk GPPCN and GPPCN nanosheets were ECL-active at both cathodic and anodic potential ranges (see Figure 2, mechanisms in eqs 1−9, and more discussion in the Supporting Information), the latter exhibited much higher ECL intensity up to 70 times (Figure S4) presumably because of the improved film quantity. Moreover, the ECL intensity of GPPCN nanosheets was stable by 10 cycles of sequential voltage scans with a relative standard deviation of 0.62% and 0.50% at the cathodic (0 to −1.6 V; Figure 1b inset) and anodic (0 to 1.4 V; Figure 1d, inset) potential ranges, respectively, implying its good reliability for ECL reactions.

$$\text{GPPCN nanosheets} + e^- \rightarrow \text{GPPCN nanosheets}^{\bullet -} \quad (1)$$

$$S_2O_8^{2-} + e^- \rightarrow SO_4^{2-} + SO_4^{\bullet -} \quad (2)$$

$$\text{GPPCN nanosheets}^{\bullet -} + SO_4^{\bullet -} \rightarrow \text{GPPCN nanosheets}^* + SO_4^{2-} \quad (3)$$

$$\text{GPPCN nanosheets}^* \rightarrow \text{GPPCN nanosheets} + h\nu \quad (4)$$

$$\text{GPPCN nanosheets} - e^- \rightarrow \text{GPPCN nanosheets}^{\bullet +} \quad (5)$$

$$TEA - e^- \rightarrow TEA^{\bullet +} \quad (6)$$

$$TEA^{\bullet +} - H^+ \rightarrow TEA^{\bullet} \quad (7)$$

DOI: 10.1021/acsami.5b07405
ACS Appl. Mater. Interfaces 2015, 7, 23672−23678

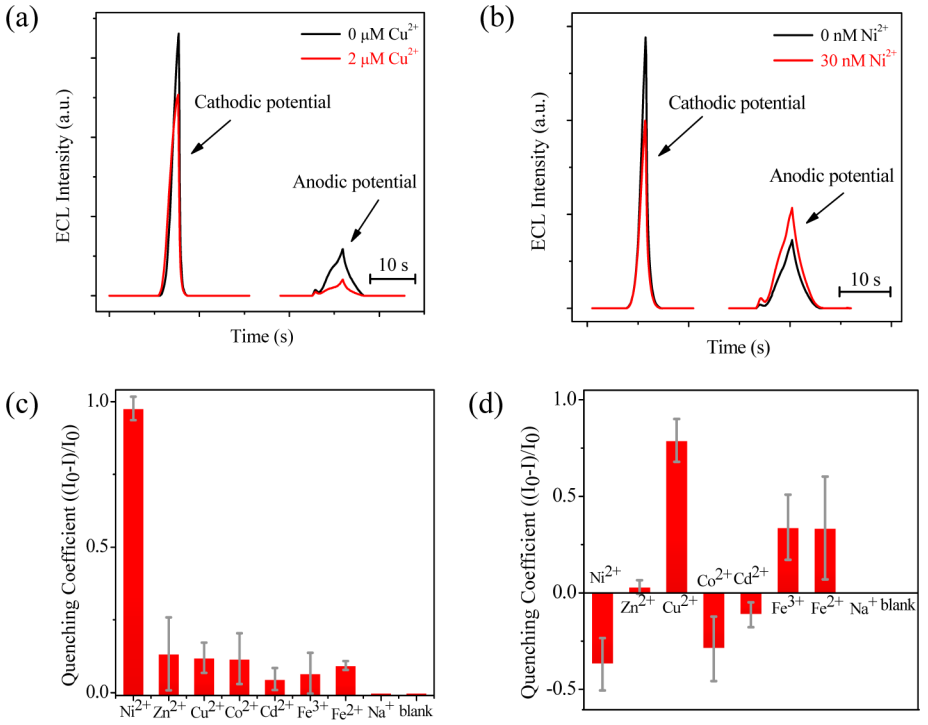

Figure 3. ECL intensity of the GPPCN-nanosheet-modified GCE before and after the addition of 2 μM Cu^{2+} ion (a) and 30 nM Ni^{2+} ion (b) in 0.01 M Tris-HCl (pH 7.4) containing 0.1 M KCl with 150 mM $K_2S_2O_8$ in the cathodic potential range and with 60 mM TEA in the anodic potential range and ECL quenching coefficient of GPPCN nanosheets after the addition of various metal ions (2 μM) in the cathodic (c) and anodic (d) potential ranges.

$$\text{GPPCN nanosheets}^{\bullet+} + \text{TEA}^{\bullet} \rightarrow \text{GPPCN nanosheets}^{*} + \text{TEA oxidant} \quad (8)$$

$$\text{GPPCN nanosheets}^{*} \rightarrow \text{GPPCN nanosheets} + h\nu \quad (9)$$

Interestingly, upon application of different electrochemical-driven potentials and the addition of various metal ions to the electrolytes, the ECL intensity of GPPCN nanosheets changed in a distinct manner. For instance, in the presence of Ni^{2+} ion, the ECL intensity decreased in the cathodic potential range and increased in the anodic potential range, while in the presence of Cu^{2+} ion, the ECL intensity decreased in both the cathodic and anodic potential ranges (Figure 3a,b). The detailed changes of the ECL signals upon other different metal ions and electrochemical potentials are plotted in Figure 3c,d. It was found that the ECL intensity decreased to different extents for most metal ions in the cathodic potential range. It could be ascribed to the fact that the redox potentials of these metal ions laid in the band gap (conduction and valence bands) of GPPCN nanosheets (Figure 4a), and the excited electrons on GPPCN nanosheets were accepted by metal ions instead of transferring back to the ground state of GPPCN nanosheets (Figure 4b); i.e., the ECL intensity in the cathodic potential range was quenched by these metal ions. Moreover, as is known for an efficient charge transfer, a proper potential difference between the energy levels of adjacent materials is generally needed. On the one hand, it should be sufficiently high with a strong driving force to perform fast charge transfer. On the other hand, it should not be very high because a high potential difference would decrease the probability of successful charge transfer because of the existence of an unwanted recombination state among them. Thus, the potential difference between the energy levels of adjacent materials should be optimized to be moderate, typically of several hundreds of millivolts. Because of the quantum confinement, the electronic band structure of the as-prepared GPPCN nanosheets differed from that of bulk or other nanostructured GPPCN (see the blue-shifted band-edge absorption and photoluminescent emission in Figure S1). Therefore, the higher quenching efficiency of Ni^{2+} ion at the cathodic potential range compared with the other ions could be ascribed to the better energy match between the conduction band of GPPCN nanosheets and the redox potential of Ni^{2+} ion, while Cu^{2+} ion was the most selectively detected using other structured GPPCN in previous reports by photo/electrochemical luminescent quenching.[15,17]

More interestingly, in the anodic potential range, the ECL intensity of GPPCN nanosheets in the presence of some specific metal ions, such as Ni^{2+}, Co^{2+}, and Cd^{2+} ions, was improved instead of the conventional quenching. The exact mechanism was not clear, but it was also observed that the electrochemical current at the GPPCN-nanosheet-modified GCE electrode increased after addition of Ni^{2+}, Co^{2+}, and Cd^{2+} ions (Figure 4c–e) during the ECL reactions, while after the addition of other metal ions such as Zn^{2+}, Cu^{2+}, Fe^{3+}, Fe^{2+}, and Na^{+} ions, it remained almost the same or decreased (Figure S5). This indicated that Ni^{2+}, Co^{2+}, and Cd^{2+} ions of similar reduction potentials (Figure 4a) accelerated one of the anodic ECL reactions (see eqs 5–9). The reactions with eqs 5 and 6 were likely prohibited by these metal ions because the Gibbs free energy of the reaction between them was positive. In this regard, enhancement of the ECL intensity of GPPCN nanosheets after the addition of Ni^{2+}, Co^{2+}, and Cd^{2+} ions was presumably due to the catalytic action of on the reaction between the GPPCN nanosheets$^{\bullet+}$ and TEA$^{\bullet}$ (eq 8).

It is worth noting that, to the best of our knowledge, such unique ECL quenching and enhancement on different metal

DOI: 10.1021/acsami.5b07405
ACS Appl. Mater. Interfaces 2015, 7, 23672–23678

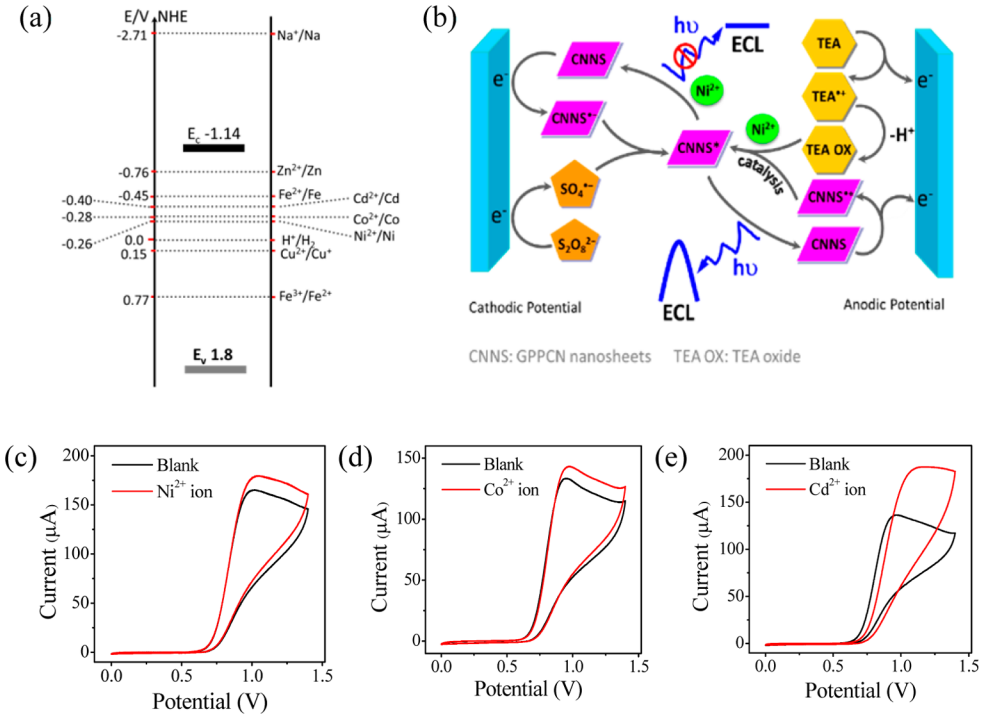

Figure 4. Chart of the electronic band structure of GPPCN nanosheets and redox potentials of different metal ions (a), the proposed ECL reactions of GPPCN nanosheets in the presence of Ni^{2+} ion (b), and a comparison of the cyclic voltammetry curves of the GPPCN-nanosheet-modified GCE before and after the addition of 2 μM Ni^{2+} ion (c), Co^{2+} ion (d), and Cd^{2+} ion (e) in the anodic potential range in 0.01 M Tris-HCl (pH 7.4) containing 0.1 M KCl in the presence of 60 mM TEA at 0.10 V/s.

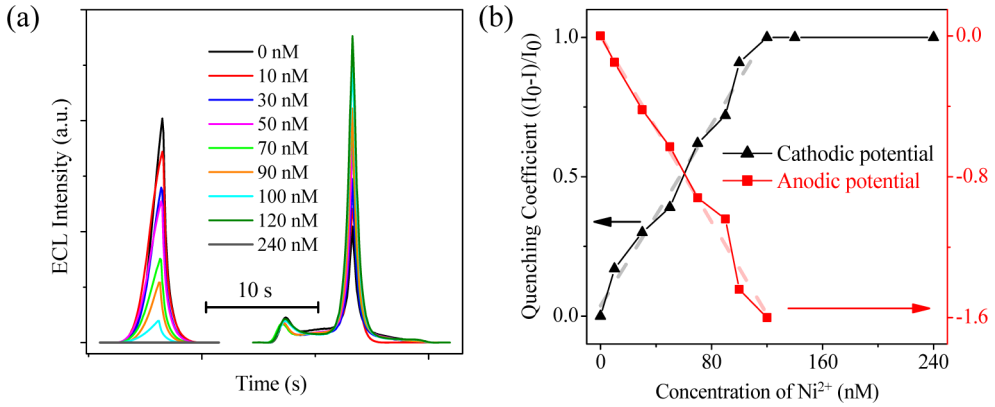

Figure 5. ECL intensity of the GPPCN-nanosheet-modified GCE with different concentrations of Ni^{2+} ion in 0.01 M Tris-HCl (pH 7.4) containing 0.1 M KCl with 150 mM $K_2S_2O_8$ at the cathodic potential range and with 60 mM TEA at the anodic potential range (a) and the linear fitting of the quenching coefficient at the cathodic and anodic potential ranges with the concentration of Ni^{2+} ion (b).

ions at different potentials (Figure 3c,d) have never been reported so far for GPPCN-based materials, although the individual cathodic[17] and anodic[18] ECL reactions of GPPCN were studied previously. On the basis of this dual-ECL signal, the interference from other metal ions to the target metal ion could be largely avoided, in principle, compared to the previous reports of a single-ECL signal.[15,17] As aforementioned, we could not distinguish which ion, Cu^{2+} or Ni^{2+}, for instance, existed in the sample according to a previous method using a single-ECL signal.[17] Nevertheless, the existence of Cu^{2+} or Ni^{2+} ion could be clarified by the changes of the second ECL signal in the anodic potential range in our method. As shown in Figure 3a,b, the ECL intensity was enhanced in the presence of Ni^{2+} ion, while that in the presence of Cu^{2+} ion decreased evidently. Thus, on the basis of the preliminary ECL "fingerprint" (quenching or enhancement at the anodic and cathodic potentials, respectively), the false-positive result could be largely avoided. Figure 5 further showed that the quenching efficiency of the ECL intensity of GPPCN nanosheets gradually changed with an increase of the concentrations of Ni^{2+} ion under the two potential ranges. Then the linear response of Ni^{2+} ion was inferred with a concentration ranging from 10 to 120 nM of a detection limit of 2.35 nM (S/N = 3) in the cathodic potential range and 1.13 nM (S/N = 3) in the anodic potential range.

To validate the reliability of the proposed analytical method in the practical samples, the content of the Ni^{2+} ion in different water samples was measured as examples, including tap water from our laboratory and Jiulong Lake water in our campus. The lake water samples were filtered through 0.22 μm membranes

DOI: 10.1021/acsami.5b07405
ACS Appl. Mater. Interfaces 2015, 7, 23672−23678

before use. The evident decrease of the ECL intensity in the cathodic potential and the increase of the ECL intensity in the anodic potential range were both observed in the lake sample, suggesting the existence of Ni^{2+} ion. As shown in Table 1, Ni^{2+} ion in the Jiulong Lake water sample was 8.83 ± 2.29 (nM), while that in the tap water was not detected. The recovery of the spiked samples obtained ranged from 95% to 103%, indicating that the present method was applicable for practical system detection.

Table 1. Result of Ni^{2+} Ion in Real Water Samples

sample	added (nM)	found (nM)	recovery (%)	RSD (%)
tap water	0	not detected		
	50	47.64 ± 8.15	95	6.89
	100	103.2 ± 28.30	103	11.04
Jiulong Lake water	0	8.83 ± 2.29		18.11
	50	57.45 ± 7.53	97	5.28
	100	109.7 ± 20.85	101	7.65

Various analytical techniques have been developed for detecting the metal ion, including chemical titration, UV spectrometry, atomic absorption spectrometry, and mass spectrometry. However, the own flaws of the detection means such as time-consuming chemical titration, poisonous dimethylglyoxime used for Ni^{2+} ion in UV spectrometry, high price and maintenance costs of the instrument for atomic absorption and mass spectrometry[47] limit their widespread application. Compared with these conventional methods, the proposed dual-ECL-signal sensing had the merits of both instrument simplicity and competitive performance. However, it should be noted that, in the current study, it was still impossible to distinguish all of the metal ions precisely and detect one metal ion quantitatively if there are several metal ions, especially that with similar ECL enhancement and quenching, such as Ni^{2+} and Cd^{2+} ions. Nevertheless, the proposed dual-ECL signals based on a single GPPCN luminophor undoubtedly provided a way to largely eliminate the negative results in sensing compared with a single cathodic ECL/photoluminescent signal in previous studies.[15,17] In addition, thanks to the band-gap engineering of GPPCN such as by chemical doping for multiple distinctive ECL signals of each metal ion[10,13] and the fitting of multiple ECL changes with the calibration curves of each metal ion, the concentration of each metal ion in a mixture could be obtained, in principle, if each metal ion changes the ECL intensity of GPPCN independently. Thus, without labeling and masking reagents, modulating different ECL reactions of GPPCN by potentials would be a promising way to develop highly selective sensors.

CONCLUSION

In summary, the dual-ECL reactions of GPPCN nanosheets were modulated simply by applying two different ranges of electrochemical potentials. Interestingly, as a single-ECL luminophor, GPPCN nanosheets exhibited unique ECL behaviors; i.e., different enhancement and quenching upon various metal ions were observed at different driven potentials. It was presumably ascribed to the diversity of energy level matches between metal ions and GPPCN nanosheets and the catalytic action of the intermediate steps of ECL reactions. Consequently, the unavoidable false-positive or -negative result using a GPPCN-nanosheet-based ECL sensor for metal ions relying on a single-ECL signal previously could be largely avoided, making the sensing more credible in principle. As an example for practical applications, the proposed GPPCN nanosheet sensor was successfully used to detect trace Ni^{2+} ion in tap and lake water by the dual-ECL signals within the single luminophor. The proposed strategy of modulating multiple-ECL signals of GPPCN would pave more reliable and promising applications of carbon-rich materials in sensing and other essential state-dependent response without labeling and masking reagents.

ASSOCIATED CONTENT

Supporting Information

The Supporting Information is available free of charge on the ACS Publications website at DOI: 10.1021/acsami.5b07405.

Figures S1−S5 and more discussions (PDF)

AUTHOR INFORMATION

Corresponding Author

*E-mail: Yuanjian.Zhang@seu.edu.cn.

Author Contributions

§These authors contributed equally.

Notes

The authors declare no competing financial interest.

ACKNOWLEDGMENTS

This work was financially supported in part by the National Natural Science Foundation of China (21203023, 91333110, and 21305065), Natural Science Foundation of Jiangsu Province (BK2012317 and BK20130788), and the Fundamental Research Funds for the Central Universities.

REFERENCES

(1) Sayari, A.; Hamoudi, S.; Yang, Y. Applications of Pore-Expanded Mesoporous Silica. 1. Removal of Heavy Metal Cations and Organic Pollutants from Wastewater. *Chem. Mater.* **2005**, *17*, 212−216.

(2) Zhang, Y.; Li, X.; Li, H.; Song, M.; Feng, L.; Guan, Y. Postage Stamp-Sized Array Sensor for the Sensitive Screening Test of Heavy-Metal Ions. *Analyst* **2014**, *139*, 4887−4893.

(3) Shen, H. M.; Zhang, Q. F. Risk Assessment of Nikel Carcinogenicity and Occupational Lung-Cancer. *Environ. Health Perspect.* **1994**, *102*, 275−282.

(4) Richter, M. M. Electrochemiluminescence (ECL). *Chem. Rev.* **2004**, *104*, 3003−3036.

(5) Miao, W. Electrogenerated Chemiluminescence and Its Biorelated Applications. *Chem. Rev.* **2008**, *108*, 2506−2553.

(6) Wu, P.; Hou, X. D.; Xu, J. J.; Chen, H. Y. Electrochemically Generated versus Photoexcited Luminescence from Semiconductor Nanomaterials: Bridging the Valley between Two Worlds. *Chem. Rev.* **2014**, *114*, 11027−11059.

(7) Liu, Z.; Qi, W.; Xu, G. Recent Advances in Electrochemiluminescence. *Chem. Soc. Rev.* **2015**, *44*, 3117−3142.

(8) Doeven, E. H.; Barbante, G. J.; Hogan, C. F.; Francis, P. S. Potential-Resolved Electrogenerated Chemiluminescence for the Selective Detection of Multiple Luminophores. *ChemPlusChem* **2015**, *80*, 456−470.

(9) Goettmann, F.; Fischer, A.; Antonietti, M.; Thomas, A. Chemical Synthesis of Mesoporous Carbon Nitrides Using Hard Templates and Their Use as a Metal-free Catalyst for Friedel-Crafts Reaction of Benzene. *Angew. Chem., Int. Ed.* **2006**, *45*, 4467−4471.

(10) Yan, S. C.; Li, Z. S.; Zou, Z. G. Photodegradation Performance of g-C_3N_4 Fabricated by Directly Heating Melamine. *Langmuir* **2009**, *25*, 10397−10401.

(11) Liu, J.; Liu, Y.; Liu, N. Y.; Han, Y. Z.; Zhang, X.; Huang, H.; Lifshitz, Y.; Lee, S. T.; Zhong, J.; Kang, Z. H. Metal-Free Efficient Photocatalyst for Stable Visible Water Splitting via a Two-Electron Pathway. *Science* **2015**, *347*, 970−974.

DOI: 10.1021/acsami.5b07405
ACS Appl. Mater. Interfaces 2015, 7, 23672−23678

(12) Wang, X.; Maeda, K.; Thomas, A.; Takanabe, K.; Xin, G.; Carlsson, J. M.; Domen, K.; Antonietti, M. A Metal-Free Polymeric Photocatalyst for Hydrogen Production from Water under Visible Light. *Nat. Mater.* **2009**, *8*, 76−80.
(13) Zhang, Y.; Antonietti, M. Photocurrent Generation by Polymeric Carbon Nitride Solids: An Initial Step towards a Novel Photovoltaic System. *Chem. - Asian J.* **2010**, *5*, 1307−1311.
(14) Lee, E. Z.; Jun, Y. S.; Hong, W. H.; Thomas, A.; Jin, M. M. Cubic Mesoporous Graphitic Carbon(IV) Nitride: An All-in-One Chemosensor for Selective Optical Sensing of Metal Ions. *Angew. Chem., Int. Ed.* **2010**, *49*, 9706−9710.
(15) Tian, J.; Liu, Q.; Asiri, A. M.; Al-Youbi, A. O.; Sun, X. Ultrathin Graphitic Carbon Nitride Nanosheet: A Highly Efficient Fluorosensor for Rapid, Ultrasensitive Detection of Cu^{2+}. *Anal. Chem.* **2013**, *85*, 5595−5599.
(16) Chen, L.; Zeng, X.; Si, P.; Chen, Y.; Chi, Y.; Kim, D. H.; Chen, G. Gold Nanoparticle-Graphite-Like C_3N_4 Nanosheet Nanohybrids Used for Electrochemiluminescent Immunosensor. *Anal. Chem.* **2014**, *86*, 4188−4195.
(17) Cheng, C.; Huang, Y.; Tian, X.; Zheng, B.; Li, Y.; Yuan, H.; Xiao, D.; Xie, S.; Choi, M. M. Electrogenerated Chemiluminescence Behavior of Graphite-Like Carbon Nitride and Its Application in Selective Sensing Cu^{2+}. *Anal. Chem.* **2012**, *84*, 4754−4759.
(18) Cheng, C.; Huang, Y.; Wang, J.; Zheng, B.; Yuan, H.; Xiao, D. Anodic Electrogenerated Chemiluminescence Behavior of Graphite-Like Carbon Nitride and Its Sensing for Rutin. *Anal. Chem.* **2013**, *85*, 2601−2605.
(19) Liu, Y.; Wang, Q.; Lei, J.; Hao, Q.; Wang, W.; Ju, H. Anodic Electrochemiluminescence of Graphitic-Phase C_3N_4 Nanosheets for Sensitive Biosensing. *Talanta* **2014**, *122*, 130−134.
(20) Wang, Q.; Wang, W.; Lei, J.; Xu, N.; Gao, F.; Ju, H. Fluorescence Quenching of Carbon Nitride Nanosheet through Its Interaction with DNA for Versatile Fluorescence Sensing. *Anal. Chem.* **2013**, *85*, 12182−12188.
(21) Zhang, X. L.; Zheng, C.; Guo, S. S.; Li, J.; Yang, H. H.; Chen, G. Turn-On Fluorescence Sensor for Intracellular Imaging of Glutathione Using g-C_3N_4 Nanosheet-MnO_2 Sandwich Nanocomposite. *Anal. Chem.* **2014**, *86*, 3426−3434.
(22) Li, R.; Liu, Y.; Cheng, L.; Yang, C.; Zhang, J. Photoelectrochemical Aptasensing of Kanamycin Using Visible Light-Activated Carbon Nitride and Graphene Oxide Nanocomposites. *Anal. Chem.* **2014**, *86*, 9372−9375.
(23) Tang, Y.; Su, Y.; Yang, N.; Zhang, L.; Lv, Y. Carbon Nitride Quantum Dots: A Novel Chemiluminescence System for Selective Detection of Free Chlorine in Water. *Anal. Chem.* **2014**, *86*, 4528−4535.
(24) Rong, M.; Lin, L.; Song, X.; Zhao, T.; Zhong, Y.; Yan, J.; Wang, Y.; Chen, X. A Label-Free Fluorescence Sensing Approach for Selective and Sensitive Detection of 2,4,6-Trinitrophenol (TNP) in Aqueous Solution Using Graphitic Carbon Nitride Nanosheets. *Anal. Chem.* **2015**, *87*, 1288−1296.
(25) Lu, Q.; Zhang, J.; Liu, X.; Wu, Y.; Yuan, R.; Chen, S. Enhanced Electrochemiluminescence Sensor for Detecting Dopamine Based on Gold Nanoflower@Graphitic Carbon Nitride Polymer Nanosheet-Polyaniline Hybrids. *Analyst* **2014**, *139*, 6556−6562.
(26) Chen, L.; Zeng, X.; Ferhan, A. R.; Chi, Y.; Kim, D. H.; Chen, G. Signal-On Electrochemiluminescent Aptasensors Based on Target Controlled Permeable Films. *Chem. Commun. (Cambridge, U. K.)* **2015**, *51*, 1035−1038.
(27) Chen, L.; Zeng, X.; Dandapat, A.; Chi, Y.; Kim, D. Installing Logic Gates in Permeability Controllable Polyelectrolyte-Carbon Nitride Films for Detecting Proteases and Nucleases. *Anal. Chem.* **2015**, *87*, 8851−8857.
(28) Zhang, Y.; Mori, T.; Ye, J. Polymeric Carbon Nitrides: Semiconducting Properties and Emerging Applications in Photocatalysis and Photoelectrochemical Energy Conversion. *Sci. Adv. Mater.* **2012**, *4*, 282−291.
(29) Dong, Y.; Chen, C.; Lin, J.; Zhou, N.; Chi, Y.; Chen, G. Electrochemiluminescence Emission from Carbon Quantum Dot-Sulfite Coreactant System. *Carbon* **2013**, *56*, 12−17.
(30) Wang, H. Y.; Xu, G. B.; Dong, S. J. Electrochemiluminescence Sensor Using Tris(2,2′-Bipyridyl)Ruthenium(II) Immobilized in Eastman-AQ55D-Silica Composite Thin-Films. *Anal. Chim. Acta* **2003**, *480*, 285−290.
(31) Kang, J. Z.; Yin, X. B.; Yang, X. R.; Wang, E. K. Electrochemiluminescence Quenching as an Indirect Method for Detection of Dopamine and Epinephrine with Capillary Electrophoresis. *Electrophoresis* **2005**, *26*, 1732−1736.
(32) Liu, X.; Niu, W.; Li, H.; Han, S.; Hu, L.; Xu, G. Glucose Biosensor Based on Gold Nanoparticle-Catalyzed Luminol Electrochemiluminescence on a Three-Dimensional Sol-Gel Network. *Electrochem. Commun.* **2008**, *10*, 1250−1253.
(33) Li, F.; Cui, H. A Label-free Electrochemiluminescence Aptasensor for Thrombin Based on Novel Assembly Strategy of Oligonucleotide and Luminol Functionalized Gold Nanoparticles. *Biosens. Bioelectron.* **2013**, *39*, 261−267.
(34) Liu, X.; Ju, H. Coreactant Enhanced Anodic Electrochemiluminescence of CdTe Quantum Dots at Low Potential for Sensitive Biosensing Amplified by Enzymatic Cycle. *Anal. Chem.* **2008**, *80*, 5377−5382.
(35) Zhao, A.; Chen, Z.; Zhao, C.; Gao, N.; Ren, J.; Qu, X. Recent Advances in Bioapplications of C-Dots. *Carbon* **2015**, *85*, 309−327.
(36) Zheng, L.; Chi, Y.; Dong, Y.; Lin, J.; Wang, B. Electrochemiluminescence of Water-Soluble Carbon Nanocrystals Released Electrochemically from Graphite. *J. Am. Chem. Soc.* **2009**, *131*, 4564−4565.
(37) Li, L.-L.; Ji, J.; Fei, R.; Wang, C.-Z.; Lu, Q.; Zhang, J.-R.; Jiang, L.-P.; Zhu, J.-J. A Facile Microwave Avenue to Electrochemiluminescent Two-Color Graphene Quantum Dots. *Adv. Funct. Mater.* **2012**, *22*, 2971−2979.
(38) Zhang, X.; Xie, X.; Wang, H.; Zhang, J.; Pan, B.; Xie, Y. Enhanced Photoresponsive Ultrathin Graphitic-Phase C_3N_4 Nanosheets for Bioimaging. *J. Am. Chem. Soc.* **2013**, *135*, 18−21.
(39) Zhang, Y.; Pan, Q.; Chai, G.; Liang, M.; Dong, G.; Zhang, Q.; Qiu, J. Synthesis and Luminescence Mechanism of Multicolor-Emitting g-C_3N_4 Nanopowders by Low Temperature Thermal Condensation of Melamine. *Sci. Rep.* **2013**, *3*, 1943.
(40) Zhang, H. R.; Xu, J. J.; Chen, H. Y. Electrochemiluminescence Ratiometry: A New Approach to DNA Biosensing. *Anal. Chem.* **2013**, *85*, 5321−5325.
(41) Li, F.; Cui, H.; Lin, X. Q. Potential-Resolved Electrochemiluminescence of $Ru(bpy)_3^{2+}/C_2O_4^{2-}$ System on Gold Electrode. *Luminescence* **2002**, *17*, 117−122.
(42) Cui, H.; Zhang, Z.-F.; Zou, G.-Z.; Lin, X.-Q. Potential-Dependent Electrochemiluminescence of Luminol in Alkaline Solution at a Gold Electrode. *J. Electroanal. Chem.* **2004**, *566*, 305−313.
(43) Shalom, M.; Gimenez, S.; Schipper, F.; Herraiz-Cardona, I.; Bisquert, J.; Antonietti, M. Controlled Carbon Nitride Growth on Surfaces for Hydrogen Evolution Electrodes. *Angew. Chem., Int. Ed.* **2014**, *53*, 3654−3658.
(44) Zhang, Y.; Thomas, A.; Antonietti, M.; Wang, X. Activation of Carbon Nitride Solids by Protonation: Morphology Changes, Enhanced Ionic Conductivity, and Photoconduction Experiments. *J. Am. Chem. Soc.* **2009**, *131*, 50−51.
(45) Zhou, Z.; Wang, J.; Yu, J.; Shen, Y.; Li, Y.; Liu, A.; Liu, S.; Zhang, Y. Dissolution and Liquid Crystals Phase of 2D Polymeric Carbon Nitride. *J. Am. Chem. Soc.* **2015**, *137*, 2179−2182.
(46) Chen, L.; Huang, D.; Ren, S.; Dong, T.; Chi, Y.; Chen, G. Preparation of Graphite-Like Carbon Nitride Nanoflake Film with Strong Fluorescent and Electrochemiluminescent Activity. *Nanoscale* **2013**, *5*, 225−230.
(47) Cui, L.; Wu, J.; Ju, H. Electrochemical Sensing of Heavy Metal Ions with Inorganic, Organic and Bio-Materials. *Biosens. Bioelectron.* **2015**, *63*, 276−286.

DOI: 10.1021/acsami.5b07405
ACS Appl. Mater. Interfaces 2015, 7, 23672−23678